CHEMICAL ENGINEERING TRANSACTIONS
VOL. 73, 2019
A publication of AIDIC
The Italian Association of Chemical Engineering
Online at www.aidic.it/cet
Guest Editors: Andrea D'Anna, Paolo Ciambelli, Carmelo Sunseri

ISBN 978-88-95608-70-9; **ISSN** 2283-9216
DOI: 10.3303/CET1973033

Continuous Removal of Cr(VI) by Lab-Scale Fixed-Bed Column Packed with Chitosan-Nanomagnetite Particles

Srikanth Vuppala[a], Angela Marchetti[b], Claudio Cianfrini[a], Marco Stoller*[b]

[a]University of Rome "La Sapienza", Dept. of Astronautics Electrical Energy Engineering, Via Eudossiana 18, 00184 Rome, Italy
[b]University of Rome "La Sapienza", Dept. of Chemical Materials Environmental Engineering Via Eudossiana 18, 00184 Rome, Italy
marco.stoller@uniroma1.it

Hexavalent Chromium species are classified as hazardous compounds due to their high toxic potential, considering also their remarkable solubility and redox potential. Various processes have been developed to remove/recover Cr(VI) species from polluted groundwater, such as membrane processes, ion-exchange and adsorption and chemical or biochemical reduction. Indeed, the reduction/removal process of Cr(VI) through iron-based materials usually leads to a pH increase of the reaction medium, allowing to facilitate the subsequent precipitation of the Cr(III) species. In this context, the use of iron based nano-particles (IBNs) supported on bio-polymer matrix allowed to maximize the Cr(VI) removal capacities of iron-based materials, leading to the production of high active and eco-compatible nano-materials. The use of chitosan as surface-modified agent, allows the reduction of aggregation forces among the produced IBNs, leading to higher surface active areas and chemical reactivity. At the same time, the use of a bio-polymer increases the eco-compatibility of the IBNs, reducing the possible interaction with bacteria and microorganisms during the treatment process. In this work chitosan-nanomagnetite particles were synthetized and employed as packing material inside fixed-bed lab-scale column (height 25 cm and diameter of 1.5 cm) to remove, in continuous, Cr(VI) species from synthetic wastewaters. The tests were performed at different inlet flow-rate values (2, 5 and 7 mL/min) at fixed Cr(VI) initial concentration (20 mg/L) and varying the solution pH (pH=4 and 7). The obtained breakthrough curves were then modeled according to the classical dynamic Thomas model.

1. Introduction

The use of nanoparticles in various sectors, such as in civil (Di Palma et al., 2015), in the cosmetic (Stoller et al., 2017a), in the catalyst-industrial (Chinh et al., 2018) and in the environmental one (Vilardi et al., 2017a) has been extensively studied, as demonstrated by the increasing number of publications on this field (Bavasso et al., 2016). Various researchers successfully tested the use of metallic nanoparticles for the removal of various pollutants, such as heavy metals (Gueye et al., 2016), organic compounds (Vilardi et al., 2018a) and inorganic anions (Muradova et al., 2016). Heavy metals pollution is considered an environmental problem of great concern (Di Palma et al., 2007) and in particular hexavalent chromium still represents a severe environmental problem in the Mediterranean Area (Vilardi et al., 2018b) since it is characterized by a high carcinogenetic and remarkable solubility and mobility in the environment. The most suitable processes for its removal are represented by adsorption (Bavasso et al., 2018), membrane treatments (Di Palma et al., 2018a), also combined with other treatments (Stoller et al., 2018a) and reduction/precipitation processes (Vilardi et al., 2018c). The adsorption process has already demonstrated its suitability for the removal and recovery of various heavy metals (Lu et al., 2017), through the use of classical or biological waste materials (Vilardi et al., 2018d). Regarding the latter process, it consists of reducing Cr(VI) to the low toxic and low soluble Cr(III) species, that usually tend to co-precipitate in mixed iron or aluminum hydroxides (Vilardi et al., 2017b). Considering the increasing necessity to develop environmentally friendly and economic technologies for a sustainable remediation procedure of polluted environments (Stoller et al., 2016), the production of nanocomposites (Stoller et al., 2018b), constituted by both organic and inorganic compounds, may play a

Paper Received: 30 March 2018; Revised: 18 September 2018; Accepted: 09 January 2019

Please cite this article as: Vuppala S., Marchetti A., Cianfrini C., Stoller M., 2019, Continuous Removal of Cr(vi) by Lab-scale Fixed-bed Column Packed with Chitosan-nanomagnetite Particles , Chemical Engineering Transactions, 73, 193-198 DOI:10.3303/CET1973033

fundamental role to reach such outstanding goals (Chinh et al., 2019). The use of iron-based nanoparticles has already proved to be very effective towards various contaminants in very complex wastewater (Vilardi et al., 2019a), such as tannery wastewaters (Vilardi et al., 2018e), heavy metals-polluted groundwater (Vilardi et al., 2018f) and in the presence of both nitrates and Cr(VI) pollutants (Maharramov et al., 2017). Therefore, the production of iron-based bio-nanocomposite represents an important field of research to develop environmentally friendly and effective materials for the removal of different pollutants in aqueous media (Vilardi and Di Palma, 2017). The aim of this work was to investigate on the removal efficiency of Cr(VI) using a bio-nanocomposite material, produced using chitosan as bio-polymer and nanomagnetite as iron based nanoparticles and employing them as packing material in lab-made column. Kinetic experiments were conducted at different inlet flow-rate values (2, 5 and 7 mL/min) at fixed Cr(VI) initial concentration (20 mg/L) and varying the solution pH (pH=4 and 7). The obtained breakthrough curves were then modeled according to the classical dynamic Thomas model, considering the mass transfer at liquid/solid interface the process limiting step (Vilardi, 2019).

2. Materials and Methods

2.1 Materials

All the reagents were purchased from Sigma Aldrich (Milan) and were of analytical grade or higher. The solutions were prepared in deionized water. The following reagents were used in the experiments: NaOH, NaCl, chitosan, K_2Cr_2O7, $FeCl_3 \cdot 6H_2O$, $FeSO_4 \cdot 7H_2O$, NH_4OH (33% v/v) Diphenylcarbazide, and H_2SO_4. The chromium salt was dissolved in deionized water to prepare a solution with an initial Cr(VI) concentration equal to 20 mg/L, whereas the NaOH and H_2SO_4 solutions were diluted up to 0.1 M and subsequently used to modify the initial Cr(VI) solution pH, measured by a Crison pH-meter (Di Palma et al., 2018b).

2.2 Bio-Nanocomposite Synthesis

The followed procedure is a modification from Tran et al. (2010), since the spinning disk reactor was used instead of classical stirred tank vessels. In brief, the iron precursors were dissolved in the aqueous chitosan solution (prepared dissolving 2 g of chitosan in 180 mL of deionized water and 20 mL of H_2SO_4 0.1 M) using a molar ratio of 2:1 among Fe(III) and Fe(II) species (0.1 M of $FeSO_4 \cdot 7H_2O$ and 0.2 M of $FeCl_3 \cdot 6H_2O$). The solution was stirred at 300 rpm for 30 min and subsequently the Chitosan-NanoMagnetite particles (CNM) were synthetized in continuous using a Spinning Disk Reactor (SDR) according to the optimal operating parameters values reported in a previous work (Vilardi et al., 2017c). The use of rotating device allows to increase mass transfer rate and to reduce the residence time inside the reactor (Di Palma and Verdone, 2009). In detail, the inlet flowrate of chitosan-iron solution was 150 mL/min, that one of NH_4OH solution was 37.5 mL/min (added according to the stoichiometric molar ratio of OH^-/Fe(II)=8 mol/mol), the injection point distance over the disk was set to 2 cm and the rotational velocity of the disk was fixed to 146.5 rad/s. The CNM particles were then characterized by Dynamic Light Scattering (Brookhaven), showing a mean dimension of 40 ± 2.5 nm. Point of Zero Charge (PZC), was determined by suspending different material amounts (0.01, 0.1, 1, 5, 10, 20 % wt) in 0.1 M NaCl solution and measuring the solution pH after 24 h of contact time, according to (Chung et al., 2012). The pH of zero charge measured was equal to 4.5, that was really close to the value of 4.8 reported by Chung et al. (2012).

2.3 Experimental set up

A borosilicate glass column of 25 cm of height and 1.5 cm of internal diameter was used in the continuous experiments (Vilardi et al., 2019b). The column was packed with 11.4 g of the CNM material to reach a bed height h (cm) of 10 cm, corresponding to a bed volume, V_b (mL), of 17.7 mL. The bed porosity, ε=0.55, was calculated as the ratio between void volume V_v (measured by the volume, mL, of the added deionized water in the packed column at the selected h, according to a previous work (Vilardi et al., 2018g)) and the related V_b. A supporting layer of 1.2 cm of glass wool was placed on the packed bed top, to prevent the sorbent floating. A peristaltic pumps (LAMBDA) was used in up-flow mode at a desired flow-rate (2, 5 and 7 mL/min), to send the Cr(VI) solution through the column (Figure 1).

Six experiments adopting the above mentioned three different inlet flow-rate values (Q (mL/min)) and two different pH value (3 and 7) were conducted to obtain the breakthrough curves for Cr(VI) compound, by fixing the sampling time to 5 min and stopping the column operation until the final Cr(VI) concentration exceeded a value of 95% of the initial Cr(VI) concentration in the synthetic solution. Once the column resulted saturated, the packing material was recovered and substituted with freshly prepared material. At selected time intervals a liquid sample was withdrawn and the CNM particles were separated through an ultra-centrifuge (14000 rpm for 5 min) and the liquid phase was withdrawn to proceed with the Cr(VI) measure through dyphenilcarbazide method (Vilardi et al., 2017b).

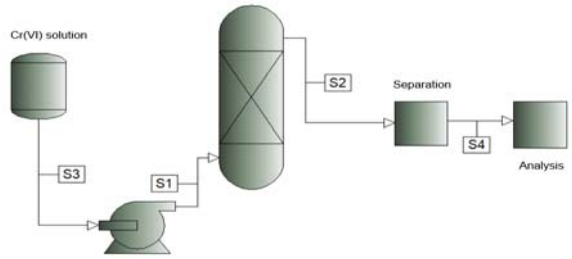

Figure 1: experimental set up scheme.

2.4 Data analysis and mathematical modeling

The breakthrough curve shape and the breakthrough time, t_b (min), are the key-parameters for the description of the column process dynamic behaviour. The former occurs when the Cr(VI) concentration in the effluent reaches a pre-determined value, usually related to the specific concentration limit for effluent disposal according to the specific environmental regulation (in this study the value of 0.2 m/L was taken into account). Another important parameter is the bed saturation time, t_e (min), that is the required process time to reach a Cr(VI) concentration in the effluent equal to $0.95Cr(VI)_0$, where the subscript 0 indicates the initial conditions. The maximum column capacity, q_{tot} (mg), is expressed by the equation reported below:

$$q_{tot} = \frac{Q}{1000}\int_{t=0}^{t=t_e} Cr(VI)_{ads}\,dt \quad (1)$$

where $Cr(VI)_{ads}$ (mg/L) is the adsorbed Cr(VI) concentration. The adsorption capacity of the column, q (mg/g), can be calculated as the ratio between q_{tot} and the CNM used mass, m(g).

The data obtained by the performed experiments were then interpreted through the dynamic Thomas model, that assumes: (i) constant separation factor and (ii) that the sorption process follows the Langmuir kinetic mechanism, occurring with negligible axial dispersion, because the process is limited by the mass transfer at the liquid/solid interface and not by the chemical reaction. The model can be described by the following equation:

$$\frac{Cr(VI)}{Cr(VI)_0} = \frac{1}{1+\exp(\frac{K_T}{Q}(q_0 m - QCr(VI)_0 t)} \quad (2)$$

where K_T (mL/min mg) is the Thomas rate constant and q_0 (mg/g) is the maximum sorption capacity of the CNM material. The data fitting was accomplished in Excel environment, using the non-linear solver function in order to avoid the errors due to linearization (White and Verdone, 2000).

3. Results and Discussion

3.1 Influence of pH and Q on process performances

Figure 2 displays the obtained breakthrough curves at different operating parameter values.

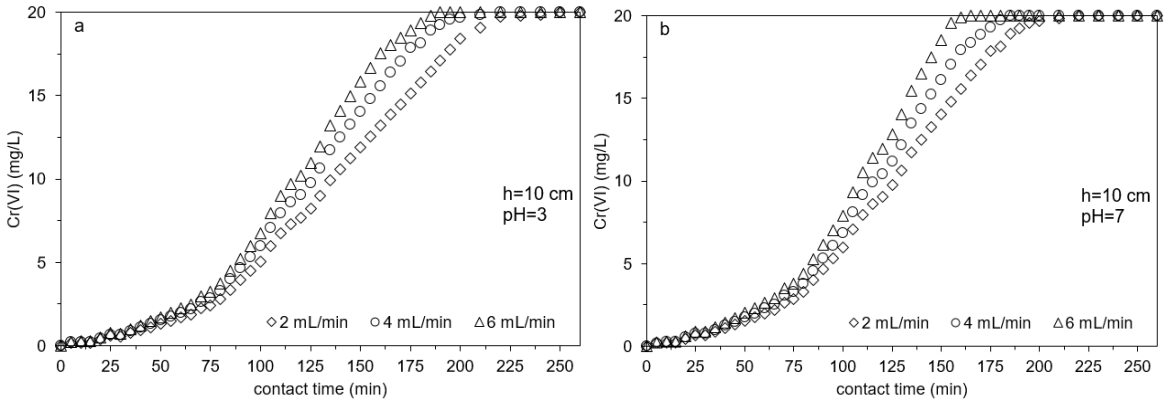

Figure 2: breakthrough curves obtained at different initial Q for pH=3 (a) and pH=7 (b) (h=10 cm, temperature=25°C, $Cr(VI)_0$=20 mg/L, the Cr(VI) concentration reported on y-axis is the Cr(VI) in the outlet of the column).

The shape of the curves changed with both pH and Q, since at higher Q the residence time among liquid phase and solid phase decreased as also reported in a previous study (Vilardi et al., 2018g) and in Table 1 (see t_e and t_b values). As a consequence, to an increase in the Q value also the t_b and t_e decreased. As regard the pH influence, it can be clearly observed from the graphs reported in figure 2, at pH=7 the curves shape slightly changed but the t_e values were substantially lower in comparison to those obtained at pH=3 (see also Table 1). The effect of pH on the Cr(VI) adsorption behavior can be explained considering the pH of zero charge: Cr(VI) compounds are present as oxyanions, thus, a positively charged surface of the adsorbent material can foster their adsorption. Since the pH of zero charge of the material is 4.5, for pH<4.5, i.e. pH=3, the surface's adsorbent resulted positively charged and the adsorption is enhanced. The chemical reduction of Cr(VI) to Cr(III) is possible onto the surface of the sorbent or in the liquid bulk, since the reducing agent is represented by the ferrous ions released by the nanoparticles or present onto the sorbent surface bonded with ferric species in the iron oxide. The reaction causes the oxidation of 3Fe(II) to 3Fe(III) and the reduction of Cr(VI) to Cr(III) species.

Table 1: parameters obtained from breakthrough data analysis ($V_{eff}=t_e*Q$ is the total effluent volume treated).

h (cm)	pH	Q (mL/min)	V_{eff} (mL)	t_e (min)	t_b (min)	q_{tot} (mg)	q_e (mg/g)
10	3	2	490	245	30	5.43	0.48
		4	860	215	20	9.53	0.84
		6	1110	185	15	13.99	1.23
	7	2	420	210	20	4.61	0.40
		4	720	180	15	9.53	0.84
		6	960	160	5	12.82	1.12

3.2 Breakthrough data fitting to Thomas model

Figure 3 shows the fitted Thomas model to the experimental data obtained at the optimal pH value.

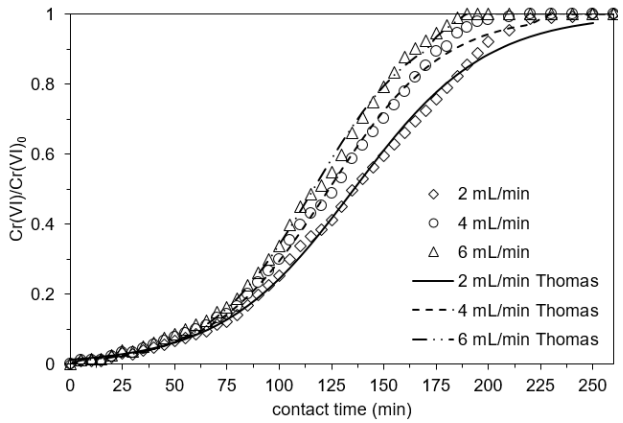

Figure 3: breakthrough curves modeling through Thomas model (pH=3, h=10 cm, temperature=25°C, $Cr(VI)_0$=20 mg/L).

Thomas model was able to well describe the breakthrough data and the asymptotic experimental behavior. The regressed model parameters are reported in Table 2, as well as the correlation coefficient values.

Table 2: regressed Thomas parameter values and correlation coefficients.

Q (mL/min)	K_T (mL/min mg)	q_0 (mg/g)	R^2
2	2.05	0.42	0.982
4			0.984
6			0.994

The obtained K_T and q_0 values are in line with those obtained in a previous study (Vilardi et al., 2018g), as expected also considering the similar breakthrough curve shapes and t_e values. The R^2 values were close to 0.99, with a higher value for the data from the experiments conducted at higher Q. However, Thomas model demonstrated to be suitable to describe the experimental behavior observed at different inlet flow-rate values.

4. Conclusions

The obtained CNM nanoparticles were tested as packing material at fixed bed height (10 cm) and varying the inlet solution pH=3 and 7, whereas the inlet flow-rate was varied as 2, 4 and 6 mL/min. The experimental results showed that the pH influenced the overall process efficiency, since for pH<pH of zero charge the adsorbent's surface resulted positively charged and the sorption of oxyanions, such as Cr(VI) species, resulted enhanced too. The increase of inlet flow-rate caused a decreased in the contact time between solid and liquid phase, causing a decrease of effluent time and, as a consequence, of the effluent treated volume. Finally, Thomas dynamic model was able to well describe the experimental data and the shape of the obtained breakthrough curves; the regressed model parameter values were in line with the expectations considering also a previous work regarding the Cr(VI) removal in more complex wastewaters.

References

Bavasso I., Vilardi G., Stoller M., Chianese A., Di Palma L., 2016, Perspectives in Nanotechnology Based Innovative Applications for The Environment, Chemical Engineering Transactions, 47, 55–60.

Bavasso I., Montanaro D., Petrucci E., Di Palma L., 2018, Shortcut Biological Nitrogen Removal (SBNR) in an MFC anode chamber under microaerobic conditions: The effect of C/N ratio and kinetic study, Sustainability, 10, 1062-1075.

Chinh V.D., Broggi A., Di Palma L., Scarsella M., Speranza G., Vilardi G., Thang P.N., 2018, XPS Spectra Analysis of Ti2+, Ti3+ Ions and Dye Photodegradation Evaluation of Titania-Silica Mixed Oxide Nanoparticles, Journal of Electronic Materials, 47, 2215–2224.

Chinh V.D., Hung L.X., Di Palma L., Hanh V.T.H., Vilardi G., 2019, Effect of Carbon Nanotubes and Carbon Nanotubes/Gold Nanoparticles Composite on the Photocatalytic Activity of TiO2 and TiO2-SiO2, Chemical Engineering and Technology, 42, 308-315.

Chung J., Chun J., Lee J., Lee S. H., Lee Y. J., Hong S. W., 2012, Sorption of Pb (II) and Cu (II) onto multi-amine grafted mesoporous silica embedded with nano-magnetite: Effects of steric factors, Journal of hazardous materials, 239, 183-191.

Di Palma L., Ferrantelli P., Merli C., Petrucci E., Pitzolu I., 2007, Influence of soil organic matter on copper extraction from contaminated soil, Soil and Sediment Contamination, 16 (3), 323-335.

Di Palma L., Verdone N., 2009, The effect of disk rotational speed on oxygen transfer in rotating biological contactors, Bioresource Technology, 100, 1467-1470.

Di Palma L., Medici F., Vilardi G., 2015, Artificial aggregate from non metallic automotive shredder residue, Chemical Engineering Transactions, 43, 1723-1728.

Di Palma L., Bavasso I., Sarasini F., Tirillò J., Puglia D., Dominici F., Torre L., 2018a, Synthesis, characterization and performance evaluation of Fe3O4/PES nano composite membranes for microbial fuel cell, European Polymer Journal, 99, 222-229.

Di Palma L., Verdone N., Vilardi G., 2018b, Kinetic Modeling of Cr(VI) Reduction by nZVI in Soil: The Influence of Organic Matter and Manganese Oxide, Bulletin of Environmental Contamination and Toxicology, 101, 692-697.

Gueye M.T., Di Palma L., Allahverdeyeva G., Bavasso I., Petrucci E., Stoller M., Vilardi G., 2016, The influence of heavy metals and organic matter on hexavalent chromium reduction by nano zero valent iron in soil, Chemical Engineering Transactions, 47, 289-294.

Lu H., Tian B., Wang J., Hao H., 2017, Montmorillonite-Supported Fe/Ni Bimetallic Nanoparticles for Removal of Cr (VI) from Wastewater, Chemical Engineering Transactions, 60, 169-174.

Maharramov A., Allahverdiyeva G., Hasanova U., Ramazanov M., Di Palma L., 2017, Synthesis and Application of Zeolite and Glass Fiber Supported Zero Valent Iron Nanoparticles as Membrane Component for Removal Nitrate and Cr (+ 6) Ions, Chemical Engineering Transactions, 60, 163-168.

Muradova G.G., Gadjieva S.R., Di Palma L., Vilardi G., 2016, Nitrates Removal by Bimetallic Nanoparticles in Water, Chemical Engineering Transactions, 47, 205–210.

Stoller M., Azizova G., Mammadova A., Vilardi G., Di Palma L., Chianese A., 2016, Treatment of Olive Oil Processing Wastewater by Ultrafiltration, Nanofiltration, Reverse Osmosis and Biofiltration, Chemical Engineering Transactions, 47, 409–414.

Stoller M., Vilardi G., Di Palma L., Chianese A., Morganti P., 2017a, Process intensification techniques for the production of nanoparticles for the cosmetic and pharmaceutical industry, Journal of Applied Cosmetology, 35 (1-2), 53-59.

Stoller M., Ochando-Pulido J.M., Vilardi G., Vuppala S., Bravi M., Verdone N., Di Palma L., 2017b, Technical and economic impact of photocatalysis as a pretreatment process step in olive mill wastewater treatment by membranes, Chemical Engineering Transactions, 57, 1171-1176.

Stoller M., Sacco O., Vilardi G., Ochando-Pulido J.M., Di Palma L., 2018a, Technical–economic evaluation of chromium recovery from tannery wastewater streams by means of membrane processes, Desalination and Water Treatment, 127, 57-63.

Stoller M., Di Palma L., Vuppala S., Verdone N., Vilardi G., 2018b, Process intensification techniques for the production of nano-and submicronic particles for food and medical applications, Current Pharmaceutical Design, 24, 2329-2338.

Tran H. V., Dai Tran L., Nguyen T. N., 2010, Preparation of chitosan/magnetite composite beads and their application for removal of Pb (II) and Ni (II) from aqueous solution, Materials Science and Engineering: C, 30(2), 304-310.

Vilardi G., Di Palma L., 2017, Kinetic Study of Nitrate Removal from Aqueous Solutions Using Copper-Coated Iron Nanoparticles, Bulletin of Environmental Contamination and Toxicology, 98 (3), 359-365.

Vilardi G., Di Palma L., Verdone N., 2017a, Competitive Reaction Modelling in Aqueous Systems: the Case of Contemporary Reduction of Dichromates and Nitrates by nZVI, Chemical Engineering Transactions, 60, 175–180.

Vilardi G., Verdone N., Di Palma L., 2017b, The influence of nitrate on the reduction of hexavalent chromium by zero-valent iron nanoparticles in polluted wastewater, Desalination and Water Treatment, 86, 252–258.

Vilardi G., Stoller M., Verdone N., Di Palma L., 2017c, Production of nano Zero Valent Iron particles by means of a spinning disk reactor, Chemical Engineering Transactions, 57, 751–756.

Vilardi G., Sebastiani D., Miliziano S., Verdone N., Di Palma L., 2018a, Heterogeneous nZVI-induced Fenton oxidation process to enhance biodegradability of excavation by-products, Chemical Engineering Journal, 335, 309–320.

Vilardi G., Ochando Pulido J.M., Verdone N., Stoller M., Di Palma L., 2018b, On the removal of Hexavalent Chromium by olive stones coated by iron-based nanoparticles: equilibrium study and Chromium recovery, Journal of Cleaner Production, 190, 200-210.

Vilardi G., Di Palma L., Verdone N., 2018c, On the critical use of zero valent iron nanoparticles and Fenton processes for the treatment of tannery wastewater, Journal of Water Process Engineering, 22C, 109–122.

Vilardi G., Di Palma L., Verdone N., 2018d, Heavy metals adsorption by banana peels micro-powder. Equilibrium modeling by non-linear models, Chinese Journal of Chemical Engineering, 26, 455-464.

Vilardi G., Rodriguez-Rodriguez J., Ochando-Pulido J.M., Verdone N., Martinez-Ferez A., Di Palma L., 2018e, Large Laboratory-Plant application of a Tannery wastewater treatment by Fenton oxidation: Fe(II) and nZVI catalyst comparison and kinetic modelling, Process Safety and Environmental Protection, 117, 629-638.

Vilardi G., Mpouras T., Dermatas D., Verdone N., Polydera A., Di Palma L., 2018f, Nanomaterials application for heavy metals recovery from polluted water: the combination of nano zero-valent iron and carbon nanotubes. Competitive adsorption non-linear modeling, Chemosphere, 201, 716-729.

Vilardi G., Ochando Pulido J.M., Stoller M., Verdone N., Di Palma L., 2018g, Fenton oxidation and chromium recovery from tannery wastewater by means of iron-based coated biomass as heterogeneous catalyst in fixed-bed columns, Chemical Engineering Journal, 351, 1-11.

Vilardi G., 2019, Mathematical modelling of simultaneous nitrate and dissolved oxygen reduction by Cu-nZVI using a bi-component shrinking core model, Powder Technology, 343, 613-618.

Vilardi G., Di Palma L., Verdone N., 2019a, A physical-based interpretation of mechanism and kinetics of Cr(VI) reduction in aqueous solution by zero-valent iron nanoparticles, Chemosphere, 220, 590-599.

Vilardi G., Rodriguez-Rodriguez J., Ochando Pulido J.M., Di Palma L., Verdone N., 2019b, Fixed-bed reactor scale-up and modelling for Cr(VI) removal using nano iron-based coated biomass as packing material, Chemical Engineering Journal, 361, 990-998.

White D. A., Verdone N., 2000, Numerical modelling of sedimentation processes, Chemical Engineering Science, 55, 2213-2222.